Acceleration Regions of the Solar Wind

Leon Ofman, Catholic University of America, NASA GSFC, Code 612.1, Greenbelt, MD 20771

Abstract: The radiation environment that can affect future manned exploration goals is formed in part by charged particles that are produced by solar disturbances, such as CME driven shocks. The solar wind magnetized plasma provides the background medium in which the shocks and energetic particles propagate. The acceleration of the solar wind close the sun in streamers and coronal holes, and the physical properties of the multi-component solar wind plasma modulate the properties of the heliospheric plasma. The acceleration of the solar wind varies on short time scale (<days) due to solar activity, and the global solar wind outflow structure varies on long time scale (years) due to the solar cycle. The results of multifluid models of the solar wind acceleration in coronal streamers, and in coronal hole are shown. The implication of the solar wind acceleration to the formation of the heliospheric plasma is discussed.

Introduction

- The solar wind shapes the magnetized plasma environment in which solar magnetic disturbances and charged particles propagate.
- IPS and SOHO observations show that the acceleration of the solar wind takes place close to the sun ($<10R_S$).
- Ulysses observation shows that the fast solar wind is relatively steady, while the slow wind is highly variable, dense (compared to fast wind) and associated with equatorial streamer belts of the solar corona (McComas et al 1997, 2000).
- The slow and fast solar wind changes dramatically on long time scales throughout the solar cycle, and on short time scales (<1day).
- Helios and Ulysses observations find Alfvénic fluctuations at 0.3 AU and >1 AU with f^{-1} spectrum in the range 10^{-6}-10^{-4}Hz and $f^{-5/3}$ at higher frequencies (Goldstein et al 1995).
- Interplanetary scintillation (IPS) measurements show significant perpendicular velocity fluctuations in the extended corona, a signature of Alfvén waves (Klinglesmith 1997; Canals et al 2002), and rapid acceleration close to the sun (Grall et al 1996).
- SOHO/UVCS observations of minor ions in coronal holes find high temperature anisotropies ($T_\perp/T_\parallel>10$) and preferential acceleration of the heavy ions over protons (Kohl et al 1997; Cranmer et al 1998).
- Low frequency MHD waves, high frequency ion-cyclotron waves, reconnection, particle beams and plasma instabilities were proposed as the sources of energy and momentum of the solar wind. However, the source of energy is still debated.
- The Solar Probe mission currently under study (McComas et al, 2005) will perform in-situ measurements of the solar wind plasma in the acceleration region, and will enable to identify the physical mechanism that lead to the acceleration of the solar wind.

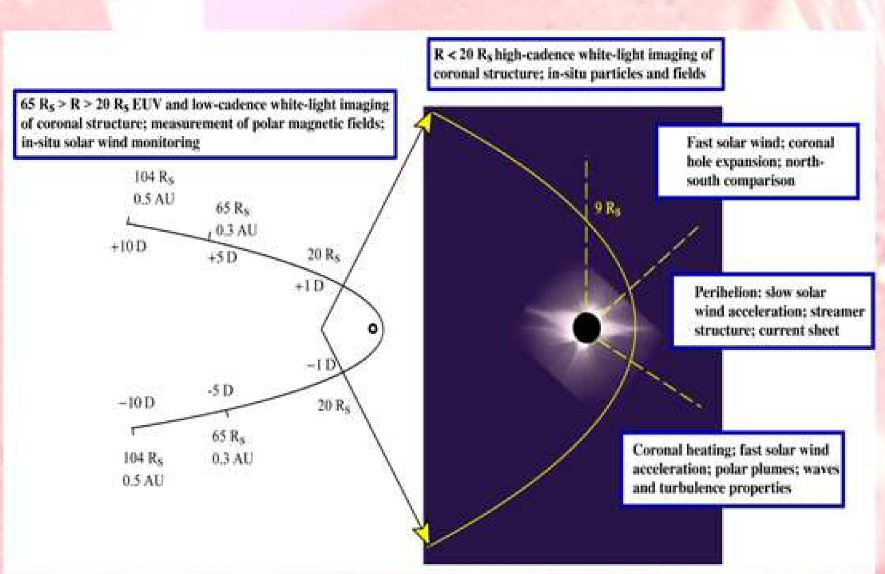

Figure 1: Solar Probe science measurements and objectives as function of orbital position. Adapted from McComas et al. 2005.

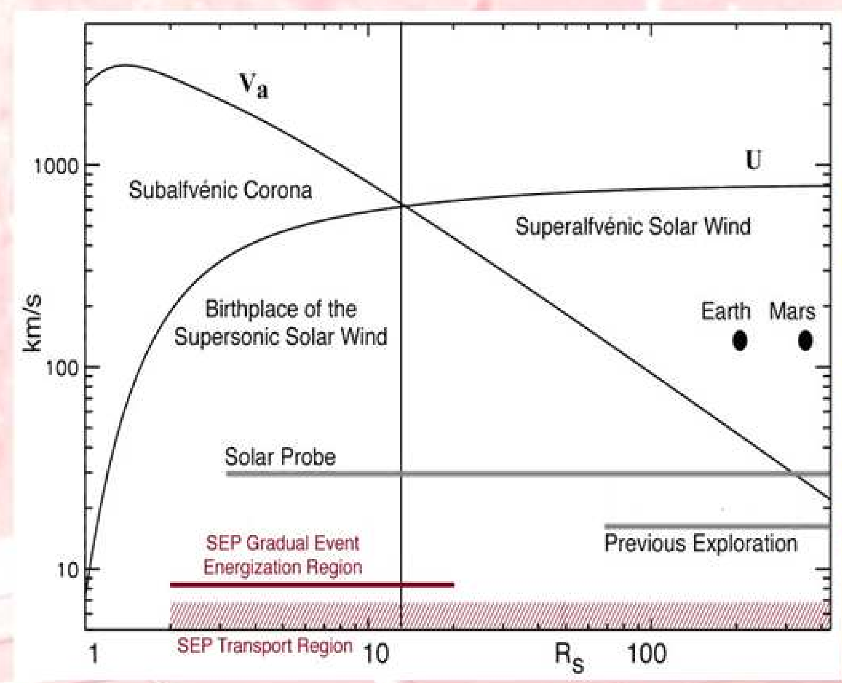

Figure 2: One-dimensional model profiles of solar wind speed and Alfvén wave speed with distance from the Sun. The vertical bar separates the source, or sub-Alfvénic, region of the wind from the supersonic solar wind flow. Solar Probe is the first mission to fly inside the solar wind source region and to sample directly the critical region of the outer corona where solar energetic particles (SEPs) are generated (McComas et al., 2005).

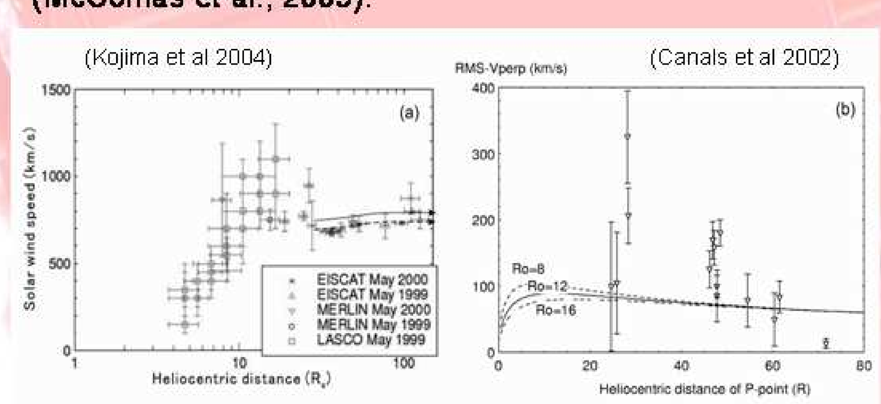

Figure 3: The solar wind acceleration and perpendicular fluctuations determined by LASCO and IPS measurements.

Three-fluid solar wind model

The normalized three fluid equations for V<<c, with gravity, resistivity, viscosity, and Coulomb friction, neglecting electron inertia, assuming quasi-neutrality are:

$$\frac{\partial n_k}{\partial t}+\nabla\cdot(n_k\mathbf{V}_k)=0, \quad (1)$$

$$n_k\left[\frac{\partial \mathbf{V}_k}{\partial t}+(\mathbf{V}_k\cdot\nabla)\mathbf{V}_k\right]=-E_{uk}\nabla p_k-E_{ue}\frac{Z_k n_k}{A_k n_e}\nabla p_e-\frac{n_k}{F_r r^2}\mathbf{e}_r$$

$$+\frac{Z_k e}{A_k m_p c}n_k(\mathbf{V}_k-\mathbf{V}_e)\times\mathbf{B}+\mathbf{F}_v+n_k\mathbf{F}_{k,coul}, \quad (2)$$

$$\frac{\partial \mathbf{B}}{\partial t}=-\nabla\times\mathbf{E},\quad \mathbf{E}=-\mathbf{V}_e\times\mathbf{B}+\frac{1}{S}\nabla\times\mathbf{B} \quad (3)$$

$$\mathbf{V}_e=\frac{1}{n_e}(n_p\mathbf{V}_p+Z_i n_i\mathbf{V}_i-b\nabla\times\mathbf{B}), \quad (4)$$

$$\frac{\partial T_k}{\partial t}=-(\gamma_k-1)T_k\nabla\cdot\mathbf{V}_k-\mathbf{V}_k\cdot\nabla T_k+C_{kjl}+(\gamma_k-1)(H_k+S_k). \quad (5)$$

where Z_k is the charge number; A_k is the atomic mass number of species ***k***, E_{uk} is the Euler number, Fr is the Froude number, $\mathbf{F}_{k,coul}$ is the Coulomb friction term, F_v is the viscous term, C_{kjl} is the thermal coupling term, H_k and S_k are loss and heating terms, and $\gamma_k=5/3$.

Wave driven fast wind in coronal holes

•The wind is driven self-consistently by the 1/*f* spectrum of Alfvén waves at $1R_S$. The waves dissipate through phase-mixing with viscous, and resistive dissipation.

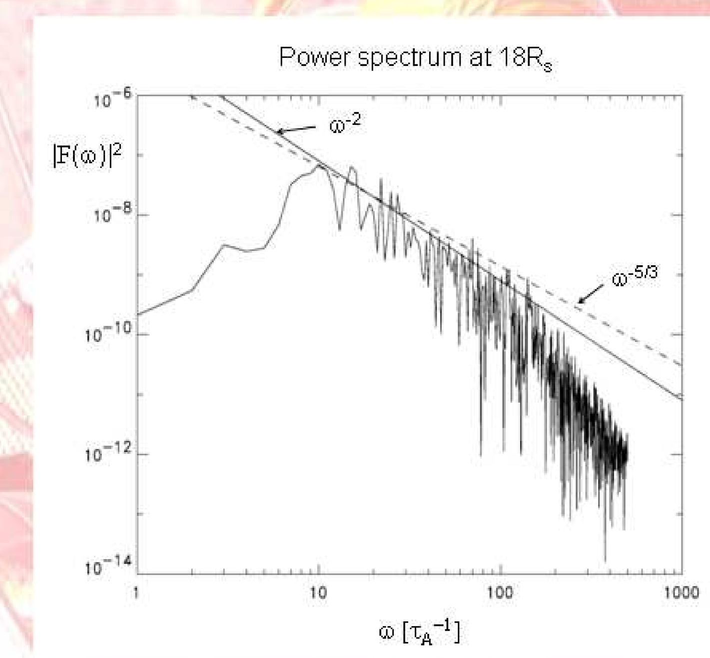

Figure 4: The power spectrum of the magnetic field fluctuations at $18R_S$ obtained in the 3-fluid model (Ofman 2004). The slope of the spectrum has increased from ω^{-1} at R_S=1. In-situ measurement of such spectrum will be possible by the Solar Probe.

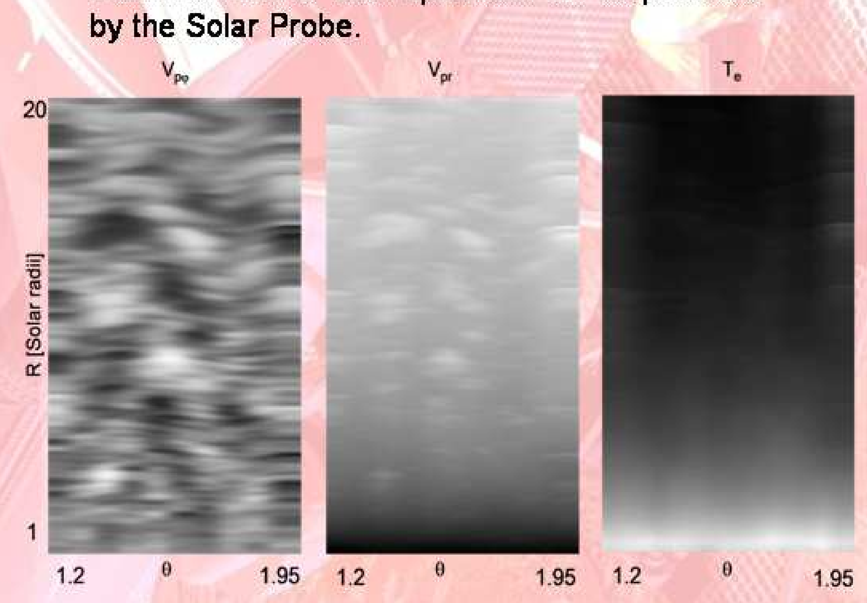

Figure 5: The proton velocity and the electron temperature in the solar wind obtained with the three-fluid model. The velocity fluctuations due to the Alfvén waves are evident in V_ϕ, and the compressive fluctuation are evident in V_r. The electron heating is in plume-like structures.

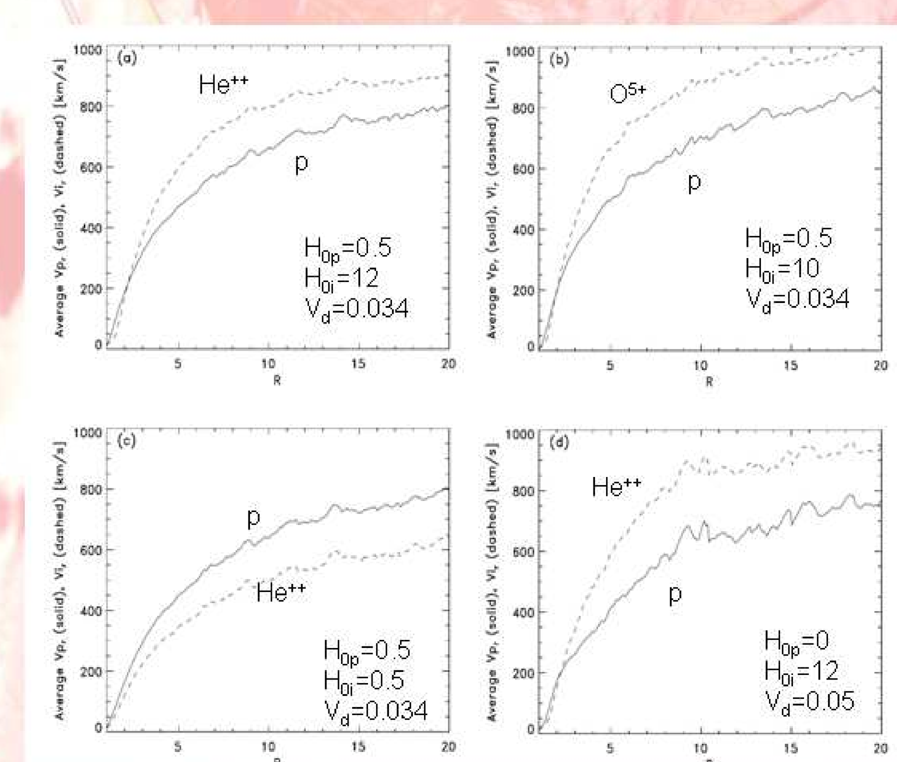

Figure 6: Results of 2.5D three fluid model of the fast solar wind in coronal holes. The outflow speed of protons (solid lines) and ions (dashed lines) in the model coronal hole averaged over θ are shown: (a) preferential (compared to protons) heating of He⁺⁺; (b) same as (a), but with O^{5+} as the heavy ions; (c) equal heat input per particle for protons and He⁺⁺ ions; (d) wave-driven wind accelerated and heated by Alfvén waves (empirical heating is included for He⁺⁺ ions only). Adapted from Ofman (2004).

Slow solar wind in streamers

The slow solar wind is modeled by adding outflowing multi-ion plasma to an initial multipole (potential) field. The model is evolved to steady state, and the streamer with the current-sheet is formed self-consistently.

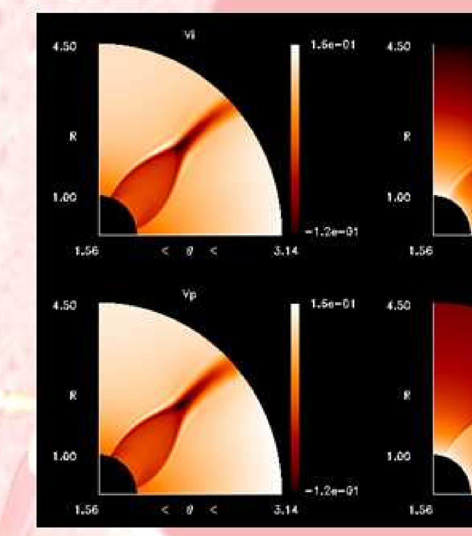

Figure 7: Three fluid model of the solar wind in streamers with polytropic energy equation (γ=1.05). The left panels show the radial outflow speed and the right panels show the He⁺⁺ (top) and protons densities.

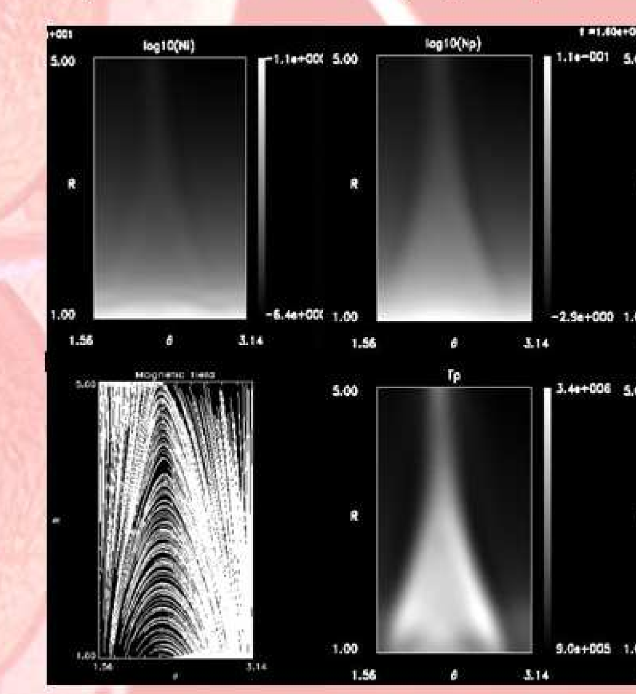

Figure 8: The results of thermally conductive three-fluid (e, p, He⁺⁺) solar wind model in a coronal streamer driven by an empirical heating function.

Conclusions

- The solar wind determines the background magnetized plasma environment in which shocks, energetic charged particles propagate. The acceleration of the solar wind plasma takes place close to the sun ($<10R_S$).
- Fast wave driven wind in coronal holes was modeled with the three-fluid code in a self-consistent model, and the different proton and heavy ions flow profiles are reproduced.
- The slow solar wind has been modeled with 2D three-fluid code, and the basic features of streamers and the different density and acceleration profiles of protons and heavy ions are reproduced.
- The study of the acceleration of the solar wind close to the sun is needed in order to characterize the heavy ion abundances in the magnetized plasma, and the radiation environments that affect space exploration.

References

1. Canals, A., A. R. Breen, L. Ofman, P. J. Moran, and R. A. Fallows: 2002, `Estimating random transverse velocities in the fast solar wind from EISCAT Interplanetary Scintillation measurements'. *Annales Geophysicae* 20, 1265.
2. Cranmer, S.R., Field, G.B., and Kohl, J. L.: 1999, `Spectroscopic Constraints on Models of Ion Cyclotron Resonance Heating in the Polar Solar Corona and High-Speed Solar Wind', *Astrophys. J.*, 518, 937
3. Goldstein, B. E., et al.: 1995, `Properties of magnetohydrodynamic turbulence in the solar wind as observed by Ulysses at high heliographic latitudes'. *Geophys. Res. Lett.* 22, 3393.
4. Grall, R. R., et al.: 1996, `Rapid acceleration of the polar solar wind'. *Nature* 379, 429.
5. Klinglesmith, M.: 1997, `The polar solar wind from 2.5 to 40 solar radii: Results of intensity scintillation measurements'. *Ph.D. Thesis, UCSD*.
6. Kohl, J. L., et al: 1997, `First Results from the SOHO Ultraviolet Coronagraph Spectrometer'. *Solar Phys.* 175, 613.
7. Kojima, M., A. R. Breen, K. Fujiki, K. Hayashi, T. Ohmi, and M. Tokumaru: 2004, `Fast solar wind after the rapid acceleration'. *J. Geophys. Res.* 109, 4103.
8. McComas, D. J., et al.: 2005, Solar Probe STDT report, NASA/TM-2005-212786.
9. McComas, D. J., et al.: 2000, `Solar wind observations over Ulysses' first full polar orbit'. *J. Geophys. Res.* 105, 10419.
10. Ofman, L.: 2004, `Three-fluid model of the heating and acceleration of the fast solar wind'. *J. Geophys. Res.* 109, 10.1029/2003JA010221.